P1.30 DEVELOPMENT OF CONVECTIVELY MIXED LAYER AND CLOUD FORMATION IN IT OBSERVED BY AN INSTRUMENTED AIRCRAFT

Masataka Murakami[1]*, Narihiro Orikasa[1], Hiroaki Horie[2], Hiroshi Kuroiwa[2], Haruya Minda[3]

1 Meteorological Research Institute, Tsukuba, Japan
2 National Institute of Information and Communications Technology, Tokyo, Japan
3 Nagoya University, Nagoya, Japan

1. INTRODUCTION

In winter, especially during cold air outbreak from the Eurasian continent, we have wide spread cloud systems over the Japan Sea.

Some cloud systems bring localized heavy snowfall over the western coast of the Japan Islands. Most of cloud systems are rather shallow and bring weak snow fall. However those shallow cloud systems are thought to be important from the view point of water and energy budgets because of their persistence and wide coverage.

In this paper, development of convective boundary layer and cloud formation in it, which were observed over the Japan Sea on 12 Feb., 2002, are documented mainly on the basis of in-situ measurements, cloud radar observations and dropsonde sounding from an instrumented aircraft (Gulfstream-II).

2. OBSERVATION FACILITIES

In the 2002 field campaign “Winter MCSs Observation over the Japan Sea in 2002 (WMO-02)”, we flew an instrumented aircraft (Galfstream-II). G-II was equipped with various kinds of cloud microphysics and ordinary meteorological instruments on the wing tip pylons. Cloud microphysics instruments included FSSP, 2D-C, 2D-P, CAPS, and two KLWC-5 probes. For measuring water vapor contents, two dewpoint hygrometers (EG&G 137) and AIR Lyman-Alpha hygrometer were used. Three components of wind relative to the ground (u, v, w) with high temporal resolution were measured by a combination of a five-hole radome with pressure transducers and Inertial Navigation System.

G-II was also equipped with w-band cloud radar, dual wavelength microwave radiometer and GPS dropsonde system. The cloud radar and microwave radiometer were installed in the pods on the left and right hand sides of fuselage. The w-band cloud radar provided us with reflectivity, Doppler velocity and polarization parameters and microwave radiometer provided us with vertically integrated liquid water amount (liquid water path: LWP).

Thus the instrumented aircraft provided us with data of microphysical, thermodynamic and kinetic structures in and around snow cloud systems.

3. SYNOPTIC FEATURES AND OBSERAVTION FLIGHT

We made an observation flight from 12 through 16 JST on 12 Feb., 2002. Winter monsoon pressure pattern, a high pressure to the west and a low to the east, was already weakened by the time (Fig.1). We observed a shallow cloud system, which is typical during late stages of cold air outbreak.

Figure 2 shows GMS IR image at 13 JST with flight track in black line and release points of GPS dropsonde by red arrows. First we flew over 300 km distance to the west-northwest at the flight level of 6.5

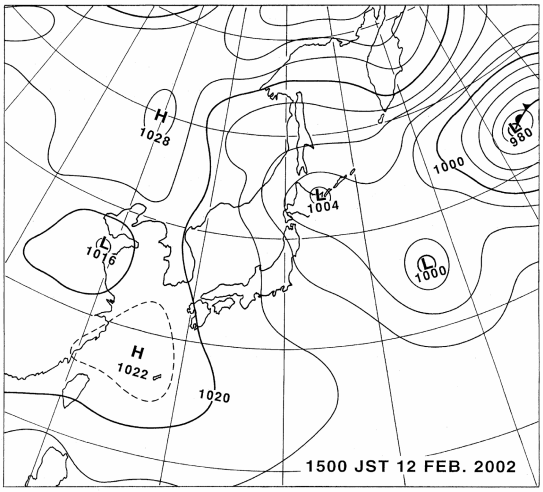

Fig. 1 Surface weather map at 15 JST on 12 Feb., 2002.

*Corresponding author’s address : Masataka Murakami, Meteorological Research Institute, Tsukuba, Ibaraki 305-0052, Japan; E-Mail: mamuraka@mri-jma.go.jp

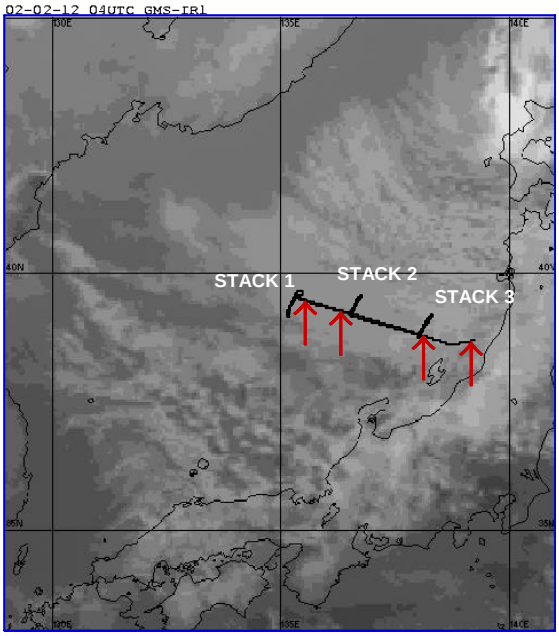

Fig.2 Flight track of G-II in black line and release points of GPS dropsonde by red arrows, superposed on GMS IR image at 13 JST on 12 Feb., 2002.

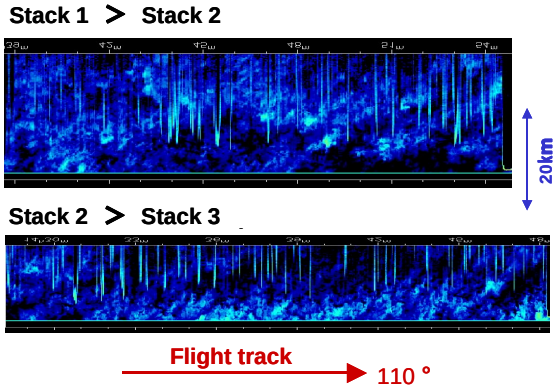

Fig. 3 Horizontal cross sections of radar reflectivity measured with w-band cloud radar during the level flights at the altitude of 300 m from STACK 1 to STACK 2 (upper) and from STACK 2 to STACK 3 (lower). Direction of flight track (110 deg.) and horizontal scale (20 km) are also indicated. Sharp white spikes extending downward from upper boundary of each panel are sea clatters due to the change of roll angles.

km. During the level flight, we made w-band cloud radar measurements in a nadir–looking mode and released GPS dropsondes at the four points.

On our way back, we made in-situ measurements in three vertical cross sections, which were oriented nearly cross-wind. Each vertical stack was made of 3 or 4 level flights. We flew at 300 m level and made cloud radar measurements in horizontal-looking mode between two adjacent vertical stacks.

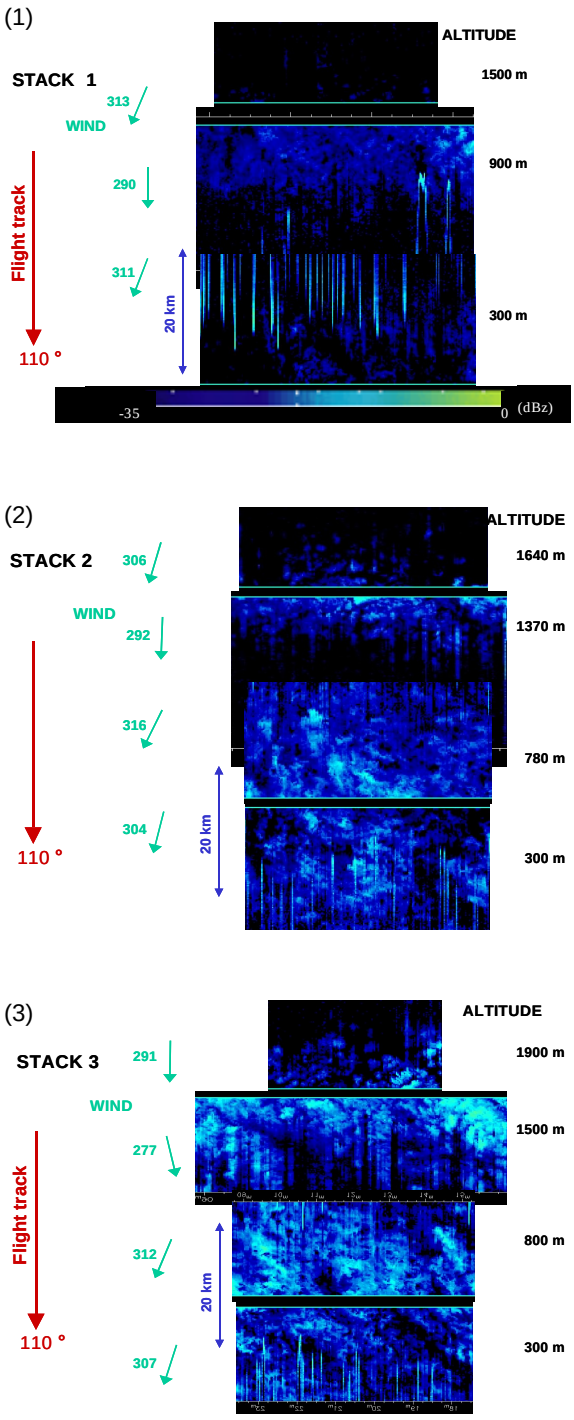

Fig. 4 Horizontal cross sections of radar reflectivity measured with w-band cloud radar during the level flights at different altitudes composing STACK 1 (panel 1), STACK 2 (panel 2) and STACK 3 (panel 3). Direction of flight track (110 deg.) and horizontal scale (20 km) are also indicated by arrows.

The shapes of cloud tops were bulky but sometimes very thin cloud layers were seen just above the bulky cloud tops.

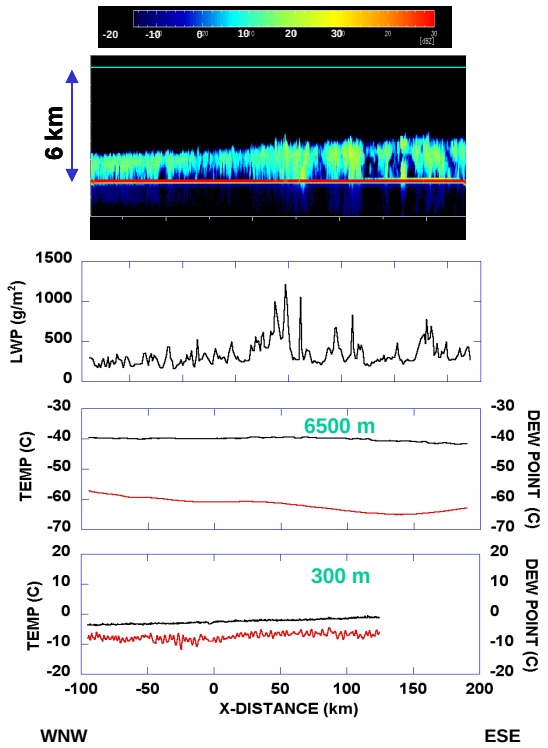

Fig. 5 Vertical cross section of cloud radar reflectivity, liquid water path measured with a microwave radiometer, air and dewpoint temperatures at 6500m and 300 m levels along the west-northwest to east-southeast flight tracks.

4. OBSERVATIONAL RESULTS

4.1 Characteristics of Shallow Cloud System

Figure 3 shows horizontal cross sections of radar reflectivity at the altitude of 300 m, measured with the cloud radar. A primary band-like structure almost parallel to the flight track, which is along the mean wind direction in cloud layer, is seen although the cloud systems did not well organize. A secondary band-like structure is also seen. Its band orientation is deviated from the mean wind direction by 50 degrees to the left. During the flight at 300 m level from upwind vertical stack (STACK 1) to mid-point vertical stack (STACK 2), aircraft seems to be located in between two primary cloud bands. On the other hand, during the flight from STACK 2 to downwind vertical stack (STACK 3), aircraft seemed to be just under a primary cloud band.

Figure 4 shows horizontal cross sections of cloud radar reflectivity taken during level flights composing STACK 1. At 1500m, just below cloud tops, very week radar echoes are seen. At 900m, the secondary band-like structure, whose band orientation is deviated from the mean wind direction to the left, became obvious. At 300 m, reflectivity became weak due to intensive evaporation (sublimation) of snow particles below cloud base.

Also at STACK 2, the similar band-like structure was seen. But by this time, precipitation had developed in clouds and significant radar echoes were

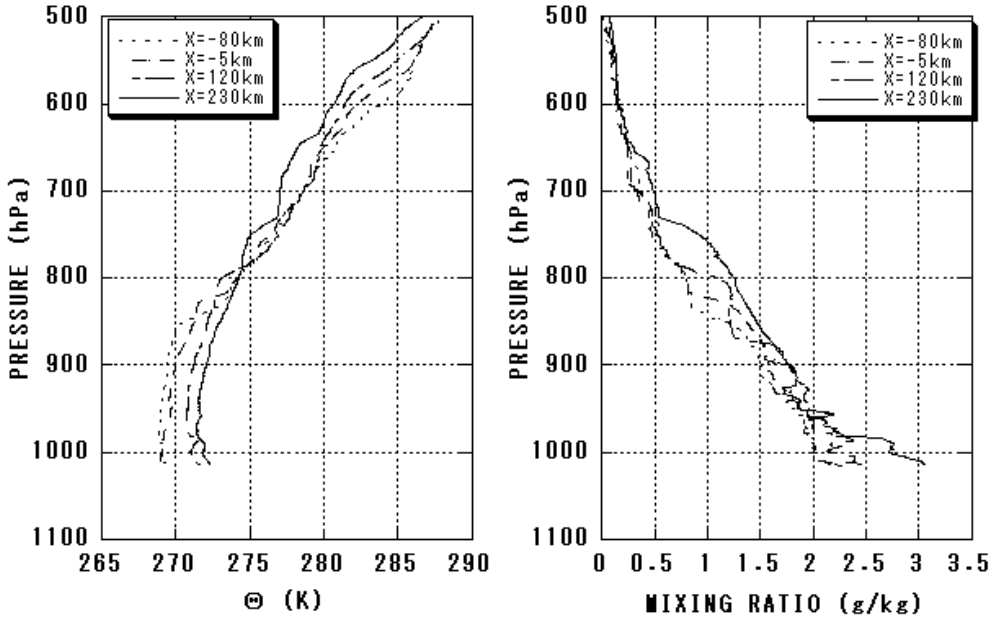

Fig. 6 Vertical profiles of potential temperature and mixing ratio measured with GPS dropsondes along the east-southeast to west-northwest flight track. Most upwind sounding is indicated by dotted (blue) line and most downwind sounding by solid (red) line.

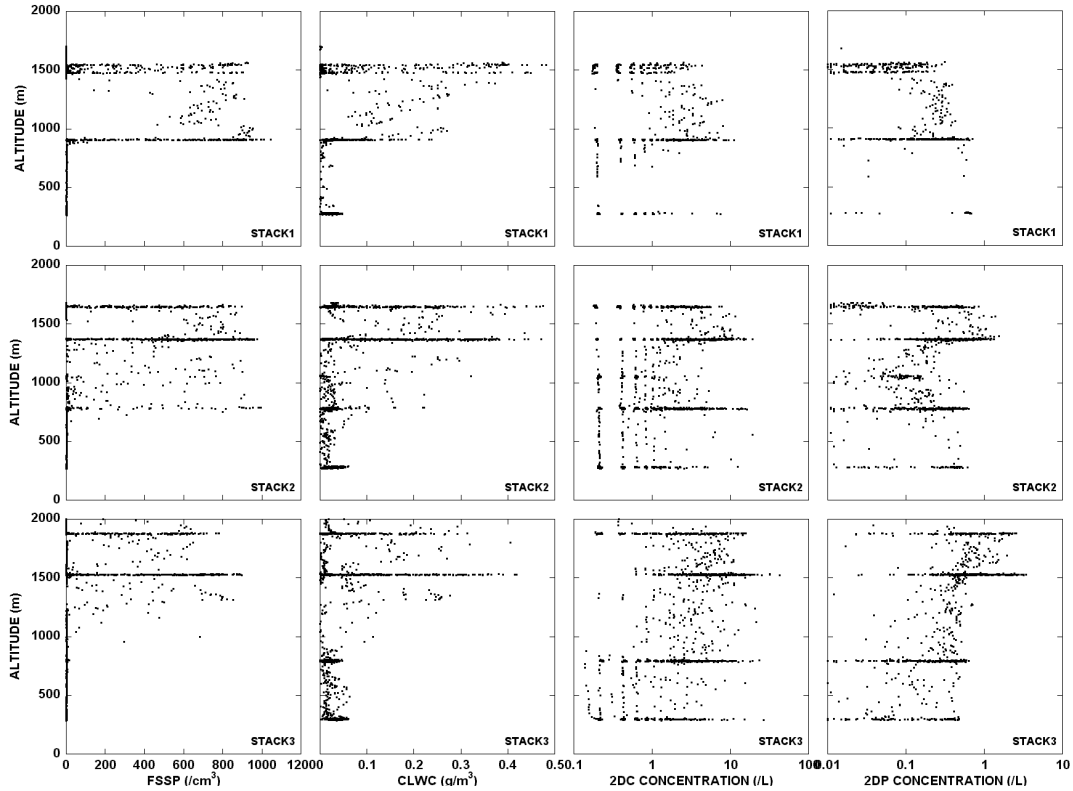

Fig. 7 Vertical profiles of microphysical variables at STACK 1 (300 km offshore), STACK 2 (200 km offshore) and STACK 3 (80 km offshore). Cloud droplet concentration, cloud water content, number concentration of ice and snow crystals larger than 25 microns and larger than 200 microns (from left to right).

observed even at 1640m, near cloud tops. Below cloud base (at 300m), radar echoes show distinct features although their reflectivity considerably decreased due to evaporation of snow particles.

At the STACK 3, strong echoes were already developed at 1900 m, and the secondary band-like structure became thick and distinct and were seen at all levels. The decrease in radar reflectivity due to evaporation of snow particles below cloud base was still obvious although reflectivity increased toward downwind at all levels. The secondary band-like structure, whose orientation was deviated from the mean wind direction by 50 degrees to the left, was almost parallel to the wind shear vector between cloud base and top.

4.2 Evolution of Convectively Mixed Boundary Layer

Vertical cross section of cloud radar reflectivity, liquid water path measured with a microwave radiometer, air and dewpoint temperatures at 6500m and 300 m levels along the west-northwest to east-southeast flight tracks are shown in Fig. 5.

Echo top height increased from 1.5 to 1.9 km and cloud top temperature decreased from –12.5 to -16 C for the traveling distance of 230 km. Radar echoes showed not only an increase in reflectivity but also a much more convective feature with the travel distance. Liquid water path gradually increased from 0.2 mm to 0.4 mm for the travel distance although liquid water path was much less than adiabatic condensation amount except for the values more than 1 mm observed in places. Air temperature at 6500 m was about –40 C and air was very dry. On the other hand, at 300 m, air temperature increased from –3 C to –0.5 C for the travel distance of 230 km. The time variation of air and dewpoint temperatures at 300 m are much more turbulent than those at 6500 m.

Vertical profiles of potential temperature and mixing ratio indicate that thickness of convective boundary layer increased from 1.5 to 1.9 km as air mass traveled over the distance of 230 km. The whole cloud layer was heated by 3 K and moistened by 0.3 gkg^{-1} (Fig. 6).

Figure 7 shows evolution of vertical profile of microphysical variables with the travel distance. Maximum number concentration of cloud droplets decreased from 1000 to 900 over the distance of 230 km. Maximum cloud water content did not change so much with the travel distance. 2DC concentration

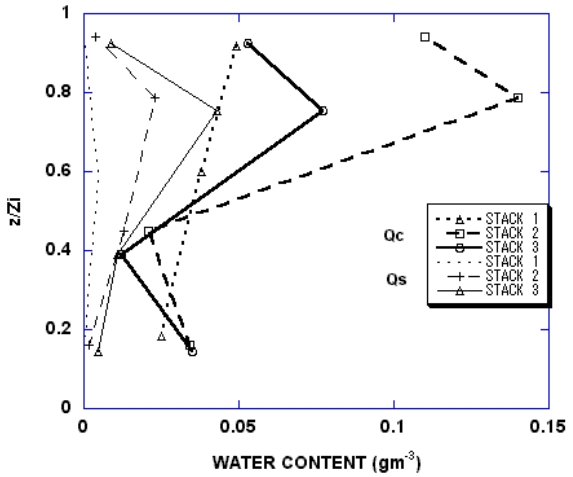

Fig. 8 Vertical profiles of cloud water and snow water contents averaged over each level flight leg at STACK 1 (dotted line), STACK 2 (dashed line), and STACK 3 (solid line).

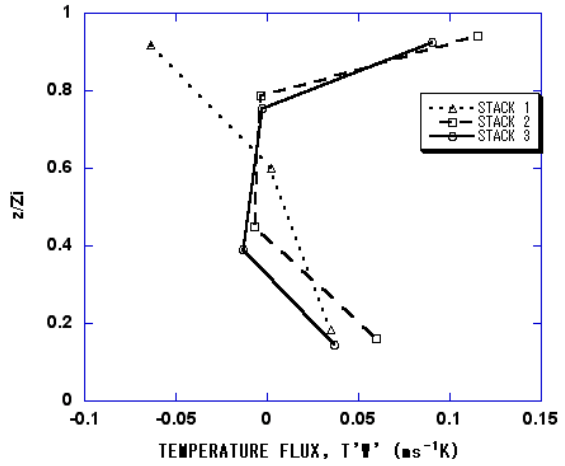

Fig. 9 Vertical profiles of temperature fluxes at STACK 1 (dotted line), STACK 2 (dashed line), and STACK 3 (solid line).

increased from 10 to 40 particles/L and 2DP concentration increased from 0.6 to 3 particles/L, being consistent with cloud radar observation. A plausible explanation for the increase in ice and snow particle concentrations is that the decrease of cloud top temperatures would promote ice nucleation rate. Typical shapes of precipitation particles changed from aggregates (dendrite), rimed crystals to heavy rimed crystals with the travel distance.

Vertical profiles of cloud water and snow water contents averaged over each level flight leg at STACK 1, 2, and 3 are shown in Fig. 8. Solid cloud bases were located around 0.5 in normalized height for each case although small amounts of cloud water were observed at locations during level flight at lower levels. Snow water content showed the tendency of monotonic increase with the travel distance. However cloud water content did not show such a monotonic increase, but showed a decrease from STACK 2 to STACK 3 due to the intensive depletion of cloud water by higher concentration of snow particles.

Snow water contents rapidly decreased below cloud base for all three vertical stacks. Reason for the rapid decrease of snow water contents is a dry air below cloud base. Relative humidity at 300m was around 60 % at all vertical stacks.

4.3 Heat and Moisture Fluxes

Temperature fluxes were calculated by eddy correlation methods, and their vertical profiles are shown in Fig. 9. Sensible heat flux was positive (upward) below cloud base and was almost zero in cloud layer. It is well known that sensible heat flux increases with height below cloud base. On the basis of this fact, surface sensible heat flux was estimated by extrapolating the observed vertical change of sensible heat fluxes below cloud base. The estimated sensible heat fluxes ranged from 100 to 130 Wm^{-2}.

Sensible heat fluxes near cloud tops showed negative value at STACK 1 and positive values at STACK 2 and 3. In general, for the case of convectively mixed, cloud-free boundary layer capped with a temperature inversion layer, sensible heat flux just above the boundary layer top would be negative, reflecting the vertical temperature profile. In the case of cloud-capped boundary layer, a shallow penetration by aircraft would result in a combination of upward transportation of colder air by overshooting cloud top and downward transportation of warmer air by compensating downdraft although a limited number of cloud top penetrations may cause a serious error in flux calculation due to a poor sampling statistics. Sensible heat flux near or just below the boundary layer top would be positive, reflecting a combination of upward transportation of warmer air in cloud parcel and downward transportation of colder air chilled by evaporative cooling due to the mixing with entrained dryer air from cloud top.

Figure 10 shows vertical profiles of moisture fluxes. The largest contribution to the net moisture fluxes came from vapor fluxes. Vapor fluxes below cloud base were almost constant and were corresponding to latent heat fluxes of 150 to 250 Wm^{-2}. In the cloud layer, a part (20 – 30 %) of upward vapor flux converted to upward liquid water flux. About one half of upward vapor flux converted to downward ice water flux in the upper and middle part of cloud layer. However, most of ice water evaporated below cloud base and only 10 -20 % of upward vapor flux returned

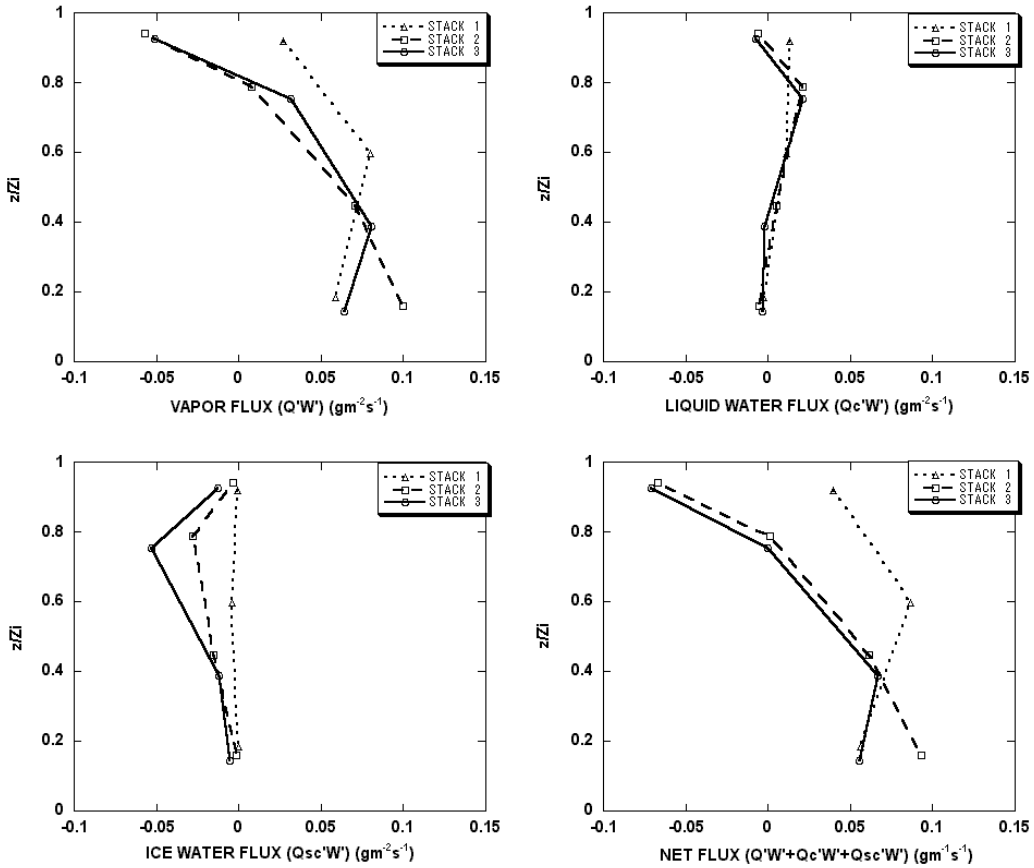

Fig. 10 Vertical profiles of water vapor flux (upper left), liquid water flux (upper right), ice water flux (lower left) and net flux (lower right) at STACK 1 (dotted line), STACK 2 (dashed line), and STACK 3 (solid line).

to sea surface in a form of precipitation. Most of water vapor and latent heat fluxes were consumed to moisten and heat the convectively mixed boundary layer and to increase ice water content in the cloud layer.

Water vapor fluxes near cloud tops showed positive value at STACK 1 and negative values at STACK 2 and 3. Upward water vapor flux at STACK 1 is easily explained in a physical sense. However a proper explanation for the downward fluxes at STACK 2 and 3 are not found for the present although downward water vapor fluxes near cloud tops have been reported in a few paper so far. Temporal changes in boundary layer structure during observation flight, influence of mesoscale convection, and poor sampling statistics due to limited length of flight legs make flux measurements susceptible to random and systematic errors.

Momentum fluxes of u (E-W wind, nearly longitudinal) and v (N-S wind, nearly lateral) components are shown as a function of height normalized by the height of boundary layer top in Fig. 11. Momentum fluxes of u component showed negative values at all levels except for near cloud top where they were close to zero. Momentum fluxes of v component were close to zero at cloud top and the lowest level and showed negative values at middle levels (in cloud layer). Both u and v components of horizontal wind have a tendency to increase with height. These observational results mean that kinetic energy of the mean wind converted to ones of disturbance (convection), being consistent with the linear theory for roll convections with their horizontal axes parallel to vertical shear of horizontal wind .

Any aircraft observations, which provide us with boundary layer development and cloud formation in it across the entire Japan Sea, have not been done so far. However composite of aircraft observations made upwind and downwind of the Japan Sea under similar synoptic weather conditions would provide us valuable insight. The case of 2 Feb., 2001 (Inoue et al., 2004) looks very similar to the present case in terms of weak winter monsoon pressure pattern and cloud feature shown in satellite images although it provides us with kinetic and thermodynamic structures, but not cloud microphysical structures. The results from the case study and the present study would envision airmass transformation processes and cloud development in

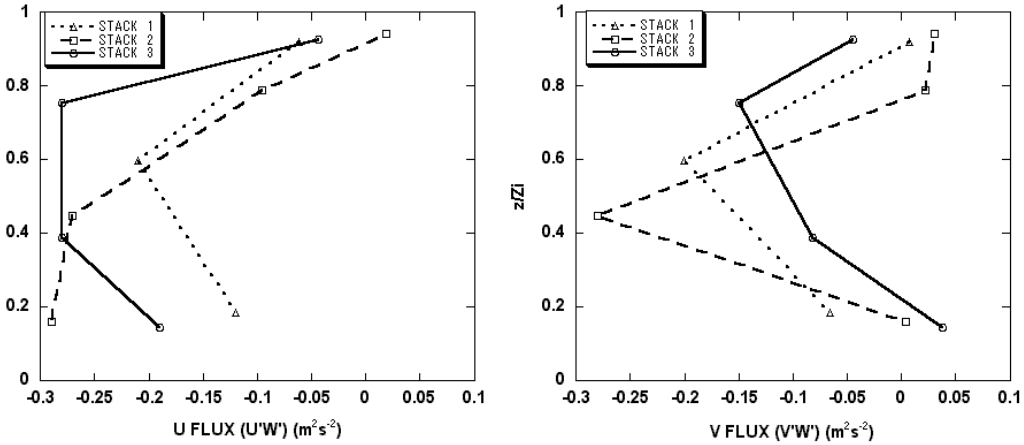

Fig. 11 Vertical profiles of u (left9 and v (right) components of momentum fluxes at STACK 1 (dotted line), STACK 2 (dashed line), and STACK 3 (solid line).

boundary layer over the entire travel distance from the east coast of the continent through the west coast of Japan Island. Sensible heat flux of 200 ~ 300 Wm^{-2} near the upwind coast decreased to 100 ~ 130 Wm^{-2} near the downwind coast of the Japan while latent heat flux increased from 100 ~ 200 to 150 ~ 250 Wm^{-2}. Consequently Bowen's ratio, defined with the ratio of latent and sensible heat fluxes, showed a decrease tendency from1.7 (upwind coast) to 0.7 (downwind coast). This is qualitatively consistent with the analytical results (Ninomiya, 1968) and 2-D numerical simulation (Murakami et al., 1994).

5. SUMMARY

Evolution of convectively mixed boundary layer and development of stratocumulus clouds in it, which were observed over the Japan Sea during late stages of cold air outbreak, are documented mainly on the basis of aircraft observation data.

Shallow convective clouds loosely organized in the form of cloud bands (or streets). The orientation of the primary band-like structure was almost parallel to the mean wind in cloud layer while the orientation of the secondary band-like structure deviated from the mean wind direction by 40 degree to the left. During the travel over a distance of 230 km, the convectively mixed layer deepened from 1.5 to 1.9 km and the whole mixed layer was heated by 3 K and moistened by 0.3 gkg^{-1}.

LWP gradually increased toward downwind although most of LWP values were much less than adiabatic condensation amount. Ice and snow particle concentrations increased downwind due to the decrease of cloud top temperature by 3.5 K. Depletion of cloud water by these ice and snow particles almost canceled an increase of LWP due to the condensation water in the mixed layer. Types of precipitation particles changed downwind from aggregates (dendrite), rimed crystals to heavy rimed crystals.

Sensible heat flux from sea surface was 100 ~ 130 Wm^{-2} while latent heat flux was 150 ~ 250 Wm^{-2}. Ice water flux (precipitation flux) near sea surface was 10 to 20 % of water vapor flux from sea surface although the maximum ice water flux in cloud layer was about one half of surface water vapor flux. This means that most of heat and water vapor fluxes were used for the development of convectively mixed boundary layer and for the increase of cloud particle concentration in stratocumulus clouds.

REFERENCES

Inoue, J., M. Kawashima, Y. Fujiyoshi, and M. Yoshizaki, 2005: Aircraft observations of air-mass modification upstream of the Sea of Japan during cold-air outbreaks. *J. Meteor. Soc. Japan*, **83**, 189-200.

Murakami, M., Terry L. Clark and William D. Hall, 1994a: Numerical Simulations of Convective Snow Clouds over the Sea of Japan; Two-Dimensional Simulations of Mixed Layer Development and Convective Snow Cloud Formation. *J. Meteor. Soc. Japan*, **72**, 43-62.

Ninomiya, K., 1968: Heat and water budget over the Japan Sea and the Japan Islands in winter season. -With special emphasis on the relation among the supply from sea surface, the convective transfer and the heavy snowfall. *J. Meteor. Soc. Japan*, **46**, 343-372.